THE JOURNAL OF BIOLOGICAL CHEMISTRY
Vol. 277, No. 44, Issue of November 1, pp. 42088–42096, 2002
Printed in U.S.A.

Constitutive Activation and Transgenic Evaluation of the Function of an *Arabidopsis* PKS Protein Kinase*

Received for publication, June 4, 2002, and in revised form, August 20, 2002
Published, JBC Papers in Press, August 26, 2002, DOI 10.1074/jbc.M205504200

Deming Gong, Changqing Zhang, Xiuyin Chen, Zhizhong Gong, and Jian-Kang Zhu‡

From the Department of Plant Sciences, University of Arizona, Tucson, Arizona 85721

A novel family of *SOS2* (salt overly sensitive 2)-like protein kinase genes (designated *PKSes*) have been recently identified in *Arabidopsis*. The biochemical characteristics as well as *in vivo* roles of most of the PKSes are unclear at present. In this work, we isolated and characterized one of the *PKSes*, *PKS18*. *PKS18* was expressed in leaves of mature *Arabidopsis* plants. The glutathione *S*-transferase (GST)-PKS18 fusion protein was inactive by itself in substrate phosphorylation. An activation loop Thr^{169} to Asp mutation, however, highly activated this kinase *in vitro* (designated PKS18T/D). Kinase activity of the PKS18T/D preferred Mn^{2+} to Mg^{2+}. The activated kinase showed a substrate specificity, and high catalytic efficiency for a peptide substrate p3 and for ATP. Interestingly, *PKS18T/D* transgenic plants were hypersensitive to the phytohormone abscisic acid (ABA) in seed germination and seedling growth, whereas silencing the kinase gene by RNA interference (RNAi) conferred ABA-insensitivity, indicating the involvement of PKS18 in plant ABA signaling.

In eukaryotic organisms, protein kinases are involved in a large number of distinct signal transduction pathways, and thus proper regulation of the catalytic activity is of crucial importance to cellular growth and development and in response to various hormonal and stress signals. In animals, calcium/calmodulin-dependent protein kinases are a major type of kinase that decode calcium signals. In plants and protists, calcium-dependent protein kinases contain a kinase catalytic domain fused with a calmodulin-like regulatory domain and are directly activated by cytosolic calcium (1, 2).

The *Arabidopsis* genome contains a large number of protein kinase genes (3). We have recently identified a novel family of 24 salt overly sensitive 2 (*SOS2*)[1]-like protein kinase genes (designated *PKSes*) from *Arabidopsis* (4, 5). The biochemical characteristics and *in vivo* roles of most of these kinases are still unknown at the present time. These PKSes are Ser/Thr protein kinases that comprise an N-terminal kinase catalytic domain similar to SNF1/AMPK and a unique C-terminal regulatory domain (4, 5). The PKS kinases can be classified into the SnRK3 subgroup of plant SNF1-related protein kinases (6). The founding member, *SOS2*, is known to function in salt tolerance in plants (4). We have also defined a novel family of SOS3-like EF-hand-type calcium sensors that may sense the calcium signal elicited by salt stress and other stimuli (5, 7, 8). SOS3 interacts with and activates SOS2 via the autoinhibitory FISL motif within the regulatory domain of SOS2 (5, 9). An up-regulation of the putative plasma membrane Na^+/H^+ antiporter *SOS1* gene by salt stress is partially controlled via *SOS2* and *SOS3* (10). Recently, both SOS3 and SOS2 have been shown to be required for the activation of Na^+/H^+ exchange activity of SOS1 (11).

Most PKS proteins, including PKS18, when expressed and isolated from bacteria, do not seem to exhibit substrate phosphorylation activity in the absence of specific SOS3-like calcium sensors. To determine the biochemical characteristics and *in vivo* roles of the novel kinases, we wanted to create constitutively active forms of these proteins. Here we isolated and characterized a novel *Arabidopsis PKS* gene, *PKS18*. *PKS18* was expressed in leaves of mature plants. Substitution of a threonine residue with aspartic acid within the activation loop resulted in a highly activated PKS18 mutant (designated PKS18T/D), suggesting an important role of the activation loop phosphorylation in the regulation of PKS18 activity. This constitutively active PKS18 mutant was then utilized to determine cofactor preference, pH dependence, substrate specificity, and kinetic properties of the kinase *in vitro*. To investigate the *in vivo* function of PKS18, we generated transgenic *Arabidopsis* plants ectopically expressing the *PKS18T/D* or dominant negative mutant by RNA interference (RNAi). *PKS18T/D* transgenic plants were hypersensitive to the phytohormone abscisic acid (ABA) in seed germination and seedling growth, whereas silencing the kinase gene via RNAi conferred ABA-insensitivity.

EXPERIMENTAL PROCEDURES

Northern Blot Analysis—Seeds of the *Arabidopsis* wild type plants (Columbia ecotype) were germinated, and seedlings were grown on Murashige and Skoog (MS) (12) agar plates under continuous light (13). Ten-day-old seedlings were treated with NaCl, cold, and drought as described previously (10, 14). Total RNA isolation and Northern blot analysis were performed as described previously (15). To analyze transgene expression, total RNA was isolated from 2-week-old seedlings grown on MS agar plates containing 0.3 μM ABA. Thirty micrograms of total RNA were used, and the blot was hybridized with a *PKS18* gene-specific DNA probe.

Reverse Transcription-Polymerase Chain Reaction and Site-directed Mutagenesis—A cDNA containing the complete open reading frame (ORF) of *PKS18* was obtained by reverse transcription (RT)-PCR. The *PKS18*-specific primers were 5′-CGGGATCCATGGATAAAAACGGCATAGTTTTGATGC-3′ (forward, *Bam*HI site underlined) and 5′-GCGGTACCTTAATGTATCACTTCAATCTTCTCATTG-3′ (reverse, *Kpn*I site underlined) (MWG-Biotech, High Point, NC). The PCR product was purified from the agarose gel, digested with *Bam*HI and *Kpn*I, and cloned into a modified pGEX-2T-CMS vector and sequenced from both strands. For analysis of the *PKS18* gene expression in wild type plants

* This work was supported by National Institutes of Health Grant R01GM59138 (to J.-K. Z.). The costs of publication of this article were defrayed in part by the payment of page charges. This article must therefore be hereby marked "*advertisement*" in accordance with 18 U.S.C. Section 1734 solely to indicate this fact.

‡ To whom correspondence should be addressed: Dept. of Plant Sciences, University of Arizona, Tucson, Arizona 85721. Tel.: 520-626-2229; Fax: 520-621-7186; E-mail: jkzhu@ag.arizona.edu.

[1] The abbreviations used are: SOS2, salt overly sensitive 2; RNAi, RNA interference; ABA, abscisic acid; AMPK, AMP-activated protein kinase; GST, glutathione *S*-transferase; MS, Murashige and Skoog; ORF, open reading frame; RT, reverse transcription; PKS, SOS2-like protein kinase; SNF1, sucrose-non-fermenting protein kinase.

and RNAi lines, the first strand cDNAs were synthesized from total RNA samples of wild type, *pks18-1, pks18-3, pks18-5,* and *pks18-8* RNAi plants. RT-PCR was performed by using the *PKS18* gene-specific primers as described above. *PKS6* and *PKS11* gene-specific primers were used in the control PCR reactions.

Site-directed mutagenesis was used to construct Thr to Asp changes or a FISL motif deletion mutant of PKS18 (designated PKS18FD). The mutagenic primers were as follows: 5′-CAAGATGGCTTGCTTCACGACACATGTGGAACACCTGC-3′ (pPKS18T/D-forward), 5′-AAGCAGGTGTTCCACATGTGTCGTGAAGCAAGCCATCTTG-3′ (pPKS18T/D-reverse), 5′-ACCGATGTCTAAAGAAGAGAGATCAGAATCGAAGTTTAC-3′ (pPKS18FD-forward), and 5′-TCTCTTCTTTAGACATCGGTTTTACGGAAAAAGCTGCGTG-3′ (pPKS18FD-reverse). PCR reactions were carried out on the plasmid DNAs with an enzyme mix (1:1) of *LA Tag* (Takara Shuzo Ltd., Kyoto) and *Pfu* Turbo DNA polymerase (Stratagene, La Jolla, CA). The gel-purified PCR products were digested with *Dpn*I and transformed into DH5α competent cells. The mutated sequences and fidelity of the rest of the DNA in these constructs were verified by sequencing.

Fusion Protein Expression and Purification—All GST fusion constructs were transformed into *Escherichia coli* BL21 codon plus cells (Stratagene). The transformed cells were grown at 37 °C in Luria-Bertani medium with ampicillin (100 μg/ml) and chloramphenicol (50 μg/ml) until the OD_{600} reached 0.8. Recombinant protein expression was induced by 0.6 mM isopropyl β-D-thiogalactopyranoside for 4 h at 37 °C. Bacterial pellets were resuspended in a phosphate-buffered saline buffer (pH 7.5) containing 10% (v/v) glycerol, 5 mM dithiothreitol, 2 μg/ml aprotinin, 2 μg/ml leupeptin, and 2 mM phenylmethylsulfonyl fluoride. GST fusion proteins were purified by glutathione-Sepharose 4B (Amersham Biosciences), and analyzed by 10% (w/v) SDS-PAGE gels.

Kinase Assays—Peptide phosphorylation with a synthetic peptide p3 (ALARAASAAALARRR, Research Genetics, Huntsville, AL) was assayed as the incorporation of radioactivity from [γ-^{32}P]ATP (PerkinElmer Life Sciences, Foster City, CA) into the peptide substrate. Kinase assay buffer contained 20 mM Tris-HCl (pH 7.2), 2.5 mM $MnCl_2$ or 5 mM $MgCl_2$, 0.5 mM $CaCl_2$, 10 μM ATP, and 2 mM dithiothreitol. Forty microliters of kinase reaction were started by adding 150 μM p3 and 5 μCi of [γ-^{32}P]ATP (specific activity of 600 cpm/pmol), and reaction mixtures were immediately incubated at 30 °C with gentle shaking for 30 min. Reactions were terminated by adding 1 μl of 0.5 M EDTA, and the glutathione-Sepharose beads were pelleted. To measure peptide phosphorylation, 15 μl of the supernatant was spotted onto P-81 phosphocellulose paper (Whatman, Clifton, NJ). The P-81 paper was washed with phosphoric acid (1%, v/v), and the phosphorylated peptide was quantified by phosphoimaging using a PhosphorImager STORM 860 (Molecular Dynamics, Sunnyvale, CA). To detect autophosphorylation, the remaining reaction mixture was separated by 10% (w/v) SDS-PAGE. The gel was dried and exposed to a Kodak x-ray film.

For determination of the divalent cation requirement, kinase assays were performed in the kinase buffer with 0–20 mM of $MnCl_2$ or $MgCl_2$, while the concentrations of p3 (150 μM) and ATP (10 μM) were fixed. To determine the effect of pH on substrate phosphorylation activity, 20 mM BIS-TRIS propane titrated to the desired pH was used in place of 20 mM Tris-HCl buffer. Peptides p1 (LRRASLG) and p2 (VRKRTLRRL) (Sigma) were also used to test the substrate specificity. Individual kinetic parameters were determined by varying the concentrations of p3 (0–300 μM) while holding ATP constant (10 μM). Alternatively, ATP concentrations were varied (0–30 μM) while keeping p3 constant (150 μM).

Transgene Constructs and Arabidopsis Transformation—To generate the overexpression construct of the *PKS18T/D* coding region, a PCR reaction was carried out using the primer sets 5′-GGGGTACCATGGATAAAAACGGCATAGTTTTGATGC-3′ (forward, *Kpn*I site underlined) and 5′-CGAGCTCTTAATGTATCACTTCAATCTTCTCATTG-3′ (reverse, *Sst*I site underlined) on the *PKS18T/D* cDNA template. The PCR product was purified from agarose gel, digested, and cloned into the binary vector, pBIB, under control of the superpromoter (16). The promoter is located upstream of the *PKS18T/D* coding region. To construct RNAi transgenic lines of *PKS18*, a gene-specific cDNA fragment was amplified by PCR using the following primer pair: 5′-CGGGATCCATTTAAATGAAGGCCTAAGCTCACGATCAC-3′ (forward, *Bam*HI and *Swa*I sites underlined) and 5′-GGACTAGTGGCGCGCCTAAATCTCCCGAAAGTC-3′ (reverse, *Spe*I and *Asc*I sites underlined). The cDNA fragment was first cloned into the pFGC1008 vector (ag.arizona.edu/chromatin/fgc1008.html) between the *Swa*I and *Asc*I sites in the antisense orientation. The sense fragment was then inserted between the *Bam*HI and *Spe*I sites. These constructs were introduced into *Agrobacterium tumefaciens* strain GV3101 and transformed into *Arabidopsis* wild type (Columbia ecotype) plants by floral infiltration (17). The dry seeds were planted on MS agar media containing hygromycin (40 mg/liter) and vancomycin (500 mg/liter), and the transgenic lines were selected. The transformed seedlings were transferred into soil to set seeds under normal growth conditions. Sterile seeds were then planted on MS agar plates, and the seeds were germinated and grown on the vertical plates at 22 °C and 16-hr light and 8-hr dark photoperiod. Seed germination and seedling growth of the wild type, T_2 and T_3 generation transgenic lines were tested on MS media for responses to various concentrations of ABA, NaCl, mannitol, sucrose, glucose, and different pH treatments. To observe ABA dose response, seeds of the transgenic and control lines were germinated and seedlings grown on MS plates containing 0, 0.15, 0.3, and 0.45 μM ABA.

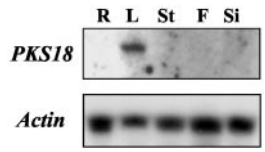

FIG. 1. **Expression of *PKS18* in different tissues of mature *Arabidopsis* plants.** Twenty micrograms of total RNA was analyzed by RNA gel blotting. The blot was hybridized with a gene-specific DNA probe for *PKS18*. The blot was exposed to an x-ray film for 7 days. *Actin* is shown as a loading control (exposed to a x-ray film for 12 h). *R*, root; *L*, leaf; *St*, stem; *F*, flower; *Si*, silique.

Data Analysis—The kinetic parameters were calculated by nonlinear least squares analysis of the averaged initial velocity data fitting to the Henri-Michaelis-Menten equation: $V_0 = V_{max} A/(K_m + A)$. In this equation, V_0 is the measured initial velocity; V_{max} is the maximum velocity; A is the substrate concentration; and K_m is the apparent Michaelis constant. The k_{cat} values were calculated by dividing V_{max} by the total enzyme concentration.

RESULTS

Expression of PKS18 in Arabidopsis Plants—A cDNA containing the ORF of *PKS18* was amplified by RT-PCR and completely sequenced. The deduced amino acid sequence of *PKS18* was identical to the computer annotation in the data base. The *PKS18* cDNA contains an ORF of 1320 bp and encodes a polypeptide of 440 amino acid residues with an estimated molecular mass of 50.2 kDa. The *PKS18* gene is located on chromosome 5 based on the *Arabidopsis* genomic sequence data base (www.arabidopsis.org). Blots of total RNA from different tissues of adult *Arabidopsis* plants were hybridized to a gene-specific DNA probe for *PKS18*. *PKS18* was expressed in leaves of adult plants, but its expression was not detectable in any of the other tissues examined (Fig. 1). We also tested potential regulation of the *PKS* gene by salt, cold, and drought in young *Arabidopsis* seedlings. *PKS18* mRNA accumulation was not significantly affected by any of the treatments (data not shown).

Substitution of a Threonine with Aspartic Acid in the Activation Loop Activates PKS18—The GST-PKS18 fusion protein in which the bacterial GST was fused in-frame to the N-terminal end of PKS18, had little kinase activity when expressed and isolated from bacteria (data not shown). To determine its biochemical characteristics, we attempted to construct constitutively active forms of the kinase. We have recently found that SOS2 could be activated either by a Thr to Asp mutation in the putative activation loop or deletion of the regulatory domain (5). Like SOS2, PKS18 contained an N-terminal SNF1-like kinase catalytic domain and a novel C-terminal regulatory domain (Fig. 2*A*). The deduced amino acid sequences of PKS18 and SOS2 were highly conserved throughout the entire length. Interestingly, PKS18 also contained a conserved putative activation loop in the catalytic domain and a FISL motif in the regulatory domain (Fig. 2*B*).

A residue, Thr^{169}, in the activation loop of PKS18 is conserved (Fig. 2*B* and data not shown). We hypothesized that the

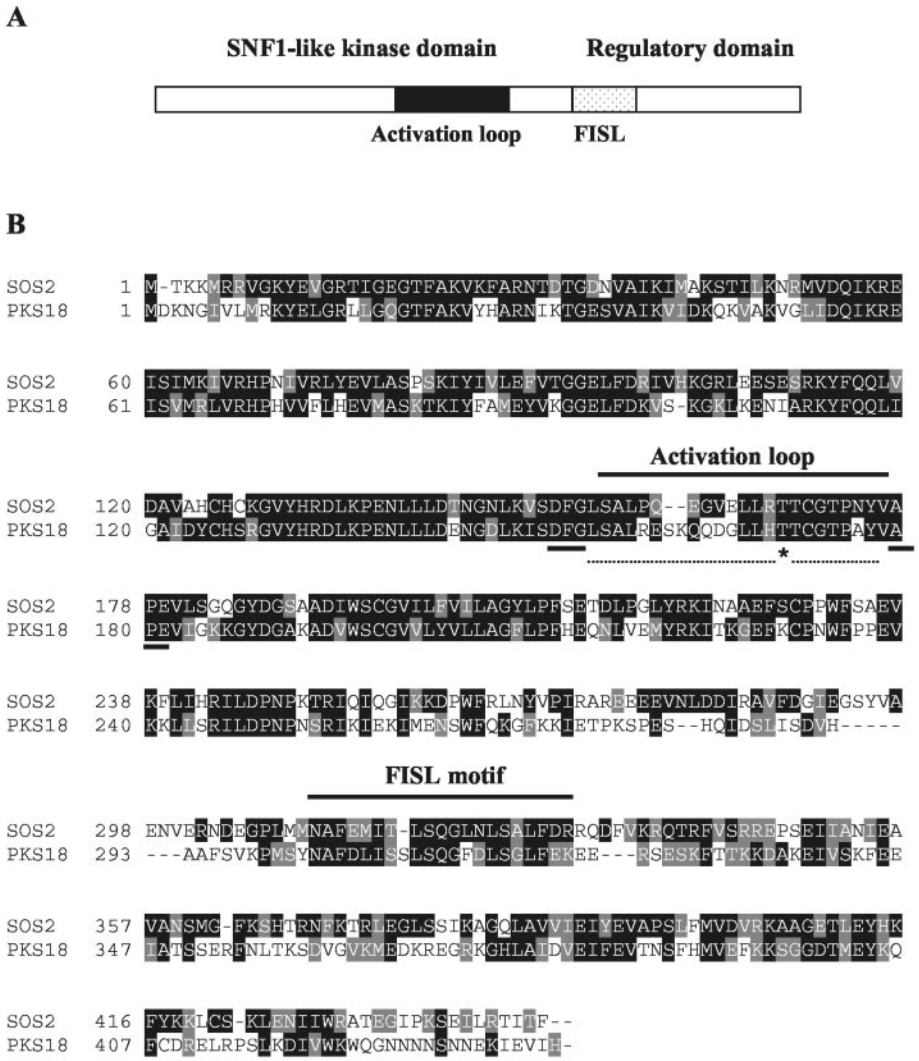

FIG. 2. **Amino acid sequence alignment of PKS18 with SOS2.** *A*, a schematic diagram of the domain structure of SOS2. *FISL*, FISL motif. *B*, an alignment of the deduced amino acids of PKS18 and SOS2. PKS18 is identical to the gene product with the GenBank™ accession number: BAB09310. Amino acids are numbered on the *left*. Identical residues and conservative replacements are shown with black and gray shading, respectively. Marked is the putative *activation loop* between the conserved DFG and APE motifs (*dots*) and the conserved Thr residue (*asterisk*). Also marked is the conserved FISL motif in the C-terminal regulatory domain. *Dashed lines* represent spaces that were introduced to maximize alignment.

threonine residue could be one critical target site for activation by a putative upstream kinase(s). We therefore substituted the residue with aspartic acid by site-directed mutagenesis to construct an activation loop mutant of PKS18 (PKS18T/D). A FISL motif deletion mutant (PKS18FD) was also produced by removing the FISL motif between Tyr^{295} and Glu^{316}. We expressed and purified the PKS18T/D and PKS18FD mutant proteins as well as the wild type protein (designated PKS18WT) from bacteria. SDS-PAGE analysis of these purified proteins showed a single band of ~80 kDa in agreement with the calculated mass (Fig. 3*A*). As shown in Fig. 3*B*, both mutant proteins exhibited higher autophosphorylation activity compared with PKS18WT. SOS2 is known to phosphorylate a synthetic peptide p3 (AMARAASAAALARRR) in the presence of SOS3 (9). With the p3 as a substrate, PKS18T/D mutant was extremely active, with a 113-fold higher activity in p3 phosphorylation than PKS18WT (Fig. 3*C*). PKS18FD also displayed a 2-fold increase in p3 phosphorylation compared with PKS18WT (Fig. 3*C*). We subsequently used the active form of PKS18, PKS18T/D, to analyze some of the biochemical properties of this kinase.

Biochemical Properties of PKS18T/D—A divalent cation is required by kinases and other phosphotransferases for coordinating the phosphate groups of the nucleotide triphosphate substrate. These enzymes may also be activated or inactivated by binding of a cation to an additional site of interaction (18). Both autophosphorylation and peptide substrate phosphorylation activities of PKS18T/D required the divalent cation Mg^{2+} or Mn^{2+} as a cofactor (Fig. 4, *A* and *B*). Interestingly, this kinase seemed to prefer Mn^{2+} to Mg^{2+} as a cofactor for either autophosphorylation or peptide phosphorylation. Mg^{2+} only weakly activated the kinase, and the activation required millimolar concentrations of Mg^{2+}, but Mn^{2+} activated the kinase even in the micromolar range. The optimal concentrations were at ~2.5 mM for Mn^{2+} and 5 mM for Mg^{2+}. Mn^{2+} concentration at 5 mM or higher became inhibitory to peptide phosphorylation activity of the kinase. In contrast, Mg^{2+} concentration up to 20 mM did not inhibit the phosphorylation activity of the kinase (Fig. 4, *A* and *B*).

P3 phosphorylation by the kinase was determined over the pH range of 6.5–9.5 (Fig. 5*A*). The optimal pH for the kinase was observed to be ~7.5, and this kinase seemed to be tolerant of slightly alkaline pH. In addition to p3, another serine-containing peptide p1 (LRRASLG) and a threonine-containing peptide p2 (VRKRTLRRL) could also be phosphorylated by SOS2 (9). Kinase assays with these three peptides showed that PKS18T/D did phosphorylate both p1 and p3, with p3 giving higher activity than p1, but it did not have any significant activity with p2 (Fig. 5*B*). To further evaluate its affinity toward the preferred peptide substrate p3 and ATP, we conducted a kinetic study for the kinase. The dependence of kinase activity of PKS18T/D on either p3 or ATP exhibited a typical Michaelis-Menten kinetics (Fig. 6, *A* and *B*). The apparent K_m values of PKS18T/D for p3 and ATP were determined to be 29

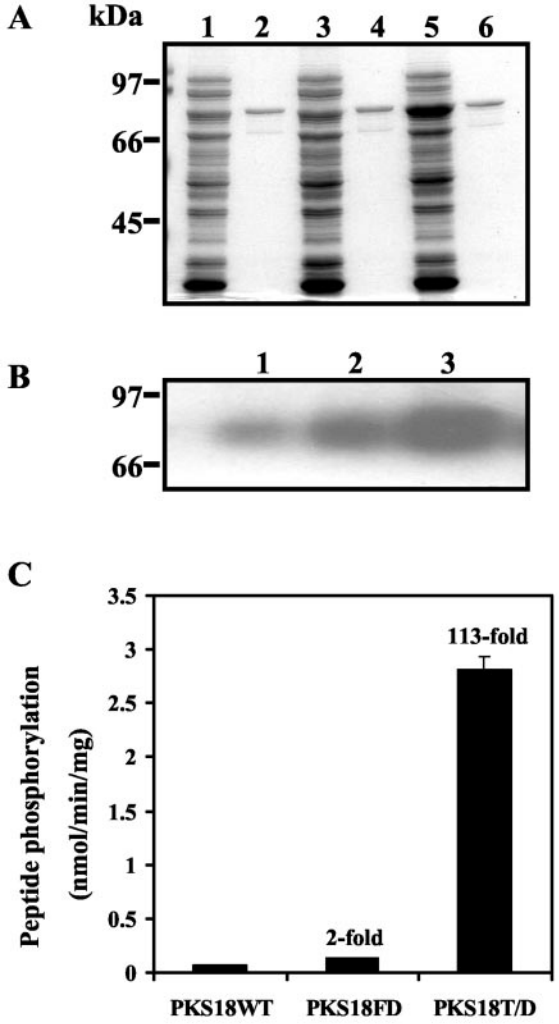

FIG. 3. **Expression of recombinant GST fusion proteins and activation of PKS18 *in vitro*.** *A*, PKS18 wild type (PKS18WT), FISL motif deletion (PKS18FD), and activation loop mutant (PKS18T/D) were expressed as GST fusion proteins in *E. coli* BL21 (codon plus), and purified by glutathione-Sepharose affinity chromatography. Expressed proteins were analyzed by SDS-PAGE, and the gels stained with Coomassie Brilliant Blue R-250. *Lanes 1*, *3*, and *5*, induced PKS18WT, PKS18FD, and PKS18T/D, respectively; *lanes 2*, *4*, and *6*, affinity-purified PKS18WT, PKS18FD, and PKS18T/D, respectively. The protein size standards were rabbit phosphorylase b (97 kDa), bovine serum albumin (66 kDa), and ovalbumin (45 kDa). *B*, autophosphorylation activities of PKS18WT (*lane 1*), PKS18FD (*lane 2*) and PKS18T/D (*lane 3*). *C*, peptide phosphorylation activities of PKS18WT, PKS18FD, and PKS18T/D. Kinase activity was assayed using 150 μM p3 as a substrate, 10 μM ATP, and 5 mM $MgCl_2$ as described under "Experimental Procedures." The number on top of each bar is a fold increase over wild type control. Results represent the means ± S.D. from three experiments.

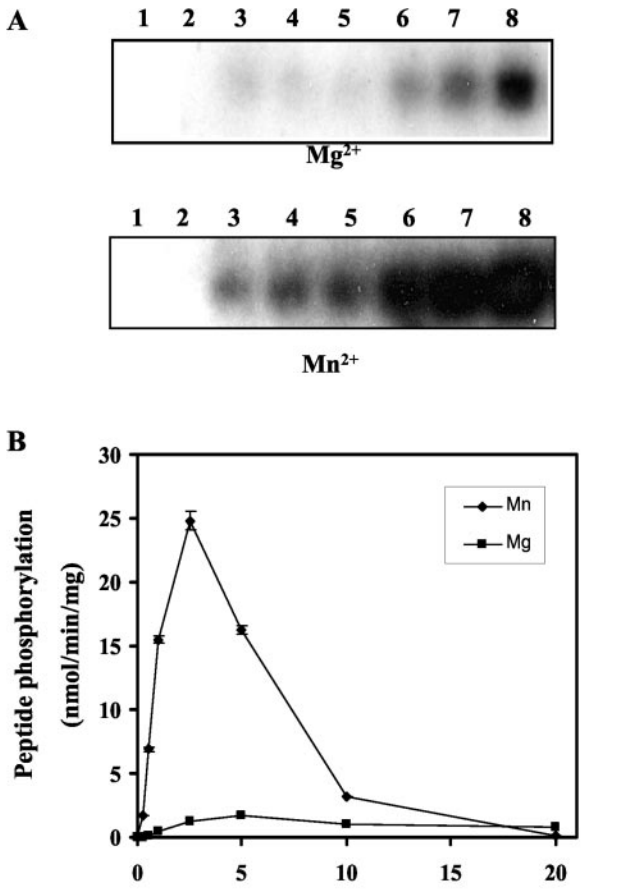

FIG. 4. **Dependence of autophosphorylation and substrate phosphorylation of PKS18T/D on divalent cation Mn^{2+} or Mg^{2+}.** *A*, autophosphorylation. Autophosphorylation of PKS18T/D in the presence of various concentrations of Mn^{2+} (as $MnCl_2$) or Mg^{2+} (as $MgCl_2$) was presented as the density of autoradiographic bands. Three independent experiments were performed, and a typical result is shown here. *Lane 1*, autophosphorylation activity with 1 mM EDTA in the kinase buffer; *lanes 2–8*, autophosphorylation activity in the presence, respectively, of 0.25, 0.5, 1.0, 2.5, 5.0, 10.0, and 20.0 mM Mn^{2+} or Mg^{2+} in the kinase assay buffer. *B*, substrate phosphorylation. Peptide p3 phosphorylation by the kinase was determined at various concentrations of Mn^{2+} (as $MnCl_2$) or Mg^{2+} (as $MgCl_2$) as indicated. Initial rates were measured and plotted against the Mn^{2+} or Mg^{2+} concentrations. Three independent experiments were performed, and the average is shown here. *Error bars* indicate ± S.D. (n = 3).

and 0.88 μM, respectively (data not shown). The ratio of k_{cat} to K_m is a good overall measure of substrate preference. The k_{cat}/K_m values of PKS18T/D for p1 and p3 were 0.76 and 2.2 M^{-1} s^{-1}, respectively (data not shown), indicating a preference of p3 over p1. In addition, the activity of PKS18T/D was slightly inhibited by high concentrations of ATP. At 25–100 μM concentrations of ATP, the activity was reduced by ~5% compared with the peak activity at 10 μM ATP. At 1 mM ATP, the kinase still had ~75% of the peak activity (data not shown).

Overexpression of PKS18T/D Confers ABA Sensitive Growth Phenotypes—SOS2 kinase is known to function in plant salt tolerance (4). To attribute *in planta* functions to PKS18, we used both gain-of-function and loss-of-function approaches. The coding region of the *PKS18T/D* was fused to the superpromoter and used to transform *Arabidopsis* plants. Over 20 T_2 and T_3 homozygous lines were recovered, and lines with high transgene expression levels were selected for more detailed analyses. The expression levels of the kinase gene in the *PKS18T/D* transgenic plants were determined by Northern blot analysis using a gene-specific probe. The results (Fig. 7*A*) showed that all the transgenic lines tested (at 0.3 μM ABA) expressed the transgene at various levels. In contrast, there was little *PKS18* transcript expression in wild type seedlings under the same conditions.

We tested the transgenic lines under various treatment conditions such as ABA, salt stress, high mannitol, sucrose or glucose, and extreme pHs. We found that the lines had a clear phenotypic change under ABA but not other treatments. To evaluate the effect of *PKS18T/D* overexpression on the ABA sensitivity in transgenic plants, seeds of the *PKS18T/D* transgenic plants were germinated and seedlings were grown on MS media containing various concentrations of ABA. When ABA concentration was 0.3 μM or higher, both seed germination and seedling growth including root growth and cotyledon greening/expansion were severely inhibited (Fig. 8*A* and data not shown). In contrast, seeds of the nontransformed wild type

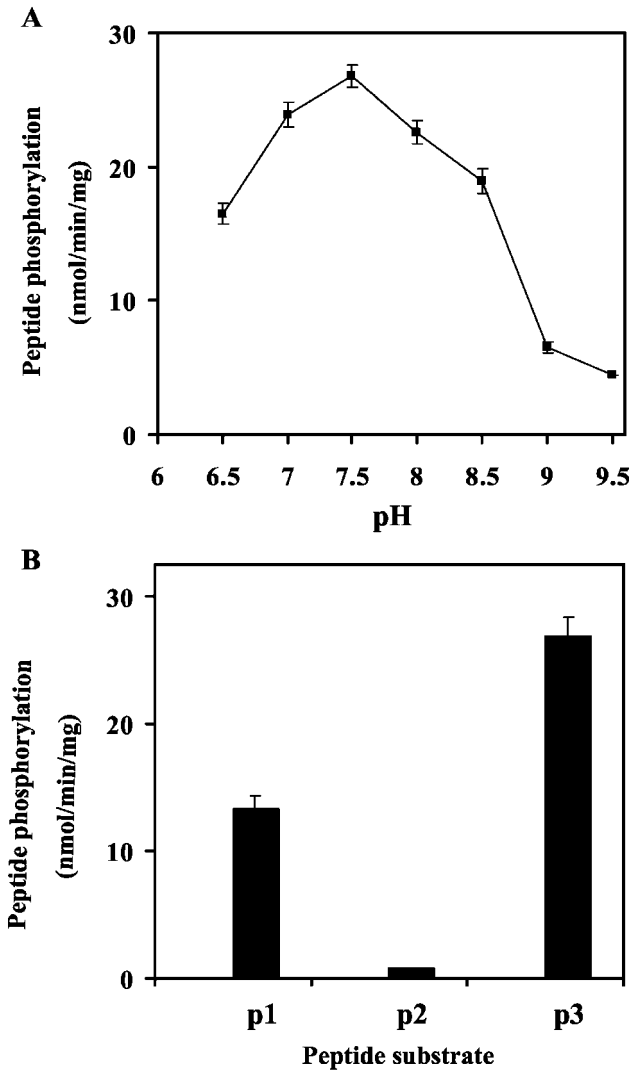

FIG. 5. **Dependence of substrate phosphorylation on assay pH and peptide substrate specificity of PKS18T/D.** *A*, pH dependence. Enzyme assays at each pH value were buffered by 20 mM BIS-TRIS propane. Kinase assays were performed at each pH value indicated. *B*, peptide substrate specificity. PKS18T/D was incubated with the kinase assay buffer containing 150 μM of each peptide substrate at 30 °C for 30 min as described under "Experimental Procedures." Each result is the mean ± S.D. from three experiments.

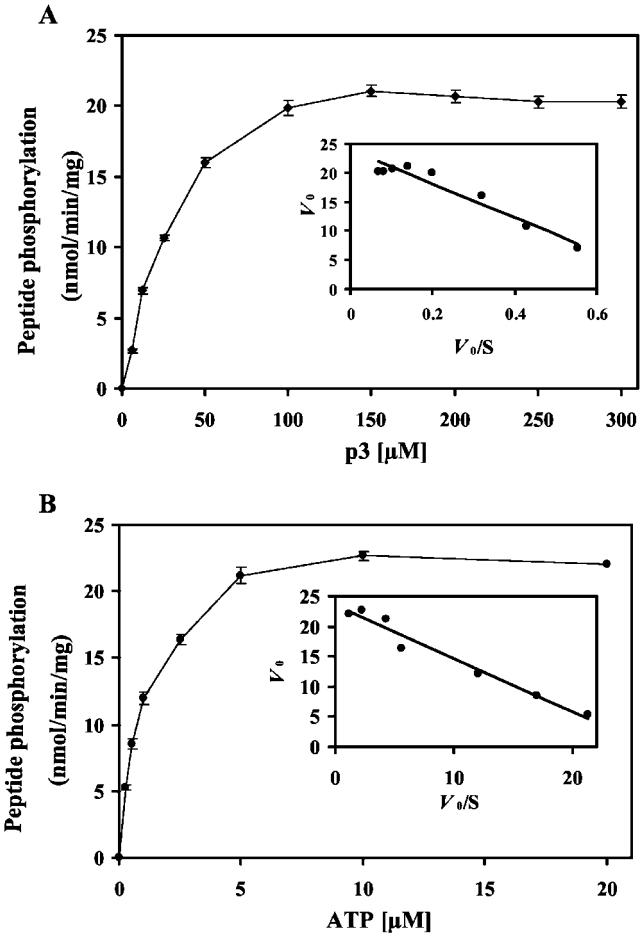

FIG. 6. **Dependence of substrate phosphorylation of PKS18T/D on peptide substrate p3 and ATP.** *A*, p3 dependence. ATP concentration in the kinase assay buffer was set constant at 10 μM. *B*, ATP dependence. P3 concentration in the kinase assay buffer was set constant at 150 μM. Phosphorylation of p3 by PKS18T/D was assayed at 30 °C in the presence of 2.5 mM $MnCl_2$ as described under "Experimental Procedures." Results shown are the averages of three independent assays presented as saturation curves with specific activity *versus* p3 or ATP concentration as indicated. The *insets* are Eadie-Hosftee plots of the average values for each data set. *Error bars* indicate ± S.D. (n = 3).

plants germinated and seedlings grew normally, although at a slower rate than on ABA-free MS media. Quantitation of seed germination (Fig. 8*B*) showed that percentage of seedlings with green cotyledons in two transgenic lines, *PKS18T*/D-1 and *PKS18T*/D-9, were only 8 and 4%, respectively, at 0.3 μM ABA, whereas the percentage in wild type plants was 55% under the same conditions. Measurement of root length showed that root growth of these two transgenic lines on 0.3 μM ABA medium was less than 20% of that on ABA-free medium (Fig. 8*C*). In contrast, root growth of wild type plants was ~70% of that on ABA-free medium.

In a dose response assay, root growth of the transgenic seedlings was found to be hypersensitive to ABA at all concentrations tested (Fig. 8*D* and data not shown). Furthermore, when young seedlings germinated on ABA-free MS plates were transferred to MS plates containing 60 or 100 μM ABA, root growth of the *PKS18T/D* transgenic lines was only ~40% of that in the wild type plants (data not shown). These observations indicated that both germination and postgermination growth of the *PKS18T/D* transgenic plants were hypersensitive to ABA.

Silencing of PKS18 Confers ABA Insensitive Growth Phenotypes—To further search the *in vivo* role of *PKS18*, we also generated dominant negative *PKS18* mutant lines (designated *pks18*) by RNAi. The expression of *PKS18* transcript was examined in 4 randomly chosen, independent *pks18* RNAi lines including *pks18-5* and *pks18-8*. The results showed that *PKS18* was silenced in all these *pks18* RNAi lines to various extents (Fig. 7*B*). Control RT-PCRs showed that expression of either the *PKS6* or *PKS11* gene that is closely related to *PKS18* (data not shown) was not affected in these *pks18* RNAi lines (Fig. 7*B*). There was no PCR product amplified from RNA samples without reverse transcription (data not shown), indicating an absence of contaminated DNA.

Over 20 independent T_2 and T_3 *pks18* RNAi lines were tested for ABA responses, and 2 representative T_3 homozygous lines (*i.e. pks18-5* and *pks18-8*) were presented here. When seeds were planted on ABA-free MS agar media, seed germination of these RNAi lines was similar to that of the wild type. However, with supplementation of 0.3 μM ABA in the media, seed germination of the *pks18* RNAi lines was earlier than the wild type (data not shown), and cotyledon greening/expansion and root growth were less inhibited as compared with the wild type (Fig. 9*A*). In these *pks18* RNAi lines, percentage of seedlings with

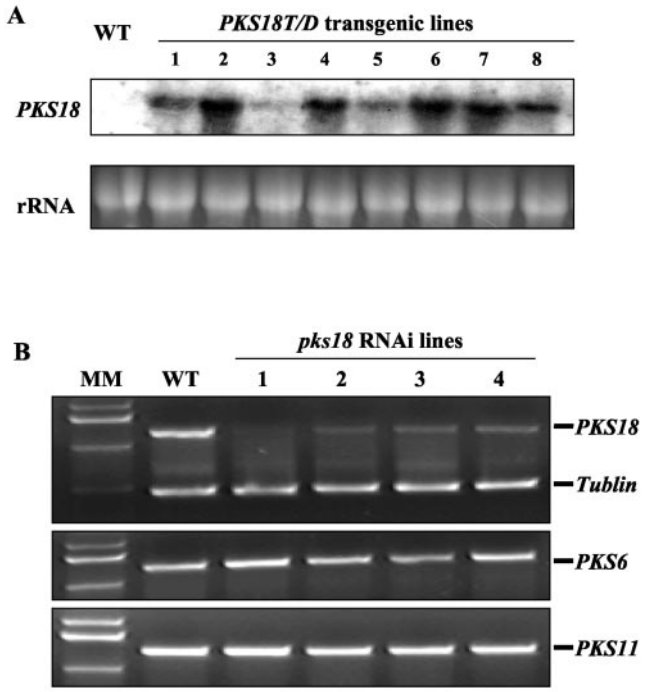

FIG. 7. **Ectopic expression of *PKS18T/D* and silencing *PKS18* gene by RNAi.** *A*, Northern blot analysis of *PKS18T/D* transgene expression. *WT*, untransformed wild type control plants; *lanes 1–8* represent transgenic lines *PKS18T/D-1*, *-2*, *-3*, *-4*, *-7*, *-8*, *-9*, and *-10*, respectively. Thirty micrograms of total RNA samples from 2-week-old seedlings grown on 0.3 μM ABA plates were used in RNA gel blot analysis. A *PKS18* gene-specific probe was used to detect *PKS18* transcript in the untransformed wild type plants (*WT*) and different transgenic lines. The Northern blot was exposed to an x-ray film for 20 h. Ethidium bromide-stained rRNA is shown as a loading control. *B*, silencing of *PKS18* gene by RNAi. *Top panel*, RT-PCR analysis with wild type plants and 4 independent *pks18* RNAi lines using *PKS18* gene-specific primers. Tubulin primers were used in the PCR reactions as an internal control. *Middle* and *bottom panel*, RT-PCR analysis with wild type plants and 4 independent *pks18* RNAi lines using *PKS6* and *PKS11* gene-specific primers, respectively. *MM*, molecular mass marker; *WT*, wild type control plants; numbers 1, 2, 3 and 4 refer to independent RNAi lines, *pks18-1*, *-3*, *-5*, and *-8*.

green cotyledons was much higher than that in the wild type on 0.3 μM ABA medium (Fig. 9*B*). Roots of these RNAi lines at 0.3 μM ABA also grew significantly better than those of the wild type (Fig. 9*C*). ABA dose response of these RNAi lines was also examined. As compared with the wild type, roots of these transgenic lines grew better under all ABA concentrations tested (Fig. 9*D*, *pks18-8* data not shown). Furthermore, root elongation of these *pks18* RNAi seedlings after transfer from ABA-free MS media was faster than the wild type on MS plates containing either 60 or 100 μM ABA (data not shown). These results suggest that both germination and postgermination growth of the *pks18* RNAi lines were less sensitive to ABA.

DISCUSSION

PKS18 is a novel leaf-specific PKS protein. The PKSes are a novel subfamily of SNF1/AMPK protein kinases. Like most kinases including SOS2, PKS18 contains a putative activation loop in the catalytic domain. In most kinases, this activation loop is phosphorylated when the kinase is active. Phosphorylation of the activation loop stabilizes it in an open conformation that is permissive for substrate binding and catalysis (19). In the present study, we found that a threonine to aspartic acid mutation in the activation loop activated PKS18 (Fig. 3). SOS2 was also activated by substitution of a threonine residue with aspartic acid in its activation loop (5). The yeast SNF1 kinase was activated by the phosphorylation of a conserved threonine residue in the activation loop of the catalytic subunit (20). These results strongly suggest that PKS18 may be activated *in vivo* through activation loop phosphorylation at the threonine residue. Two residues, Ser^{744} and Ser^{748}, in the activation loop of protein kinase D were phosphorylated during its activation (21). The use of site-specific antibodies identified a serine, Ser^{876}, within the C-terminal region of human protein kinase D2 as a phosphorylation site (22). PKS18 contains a serine residue that is absolutely conserved in the activation loop of the *Arabidopsis* PKSes (Fig. 2*B* and data not shown). It remains to be determined whether PKS18 can also be activated by substitution of the serine residue with aspartic acid or glutamic acid.

Protein kinases have diverse responses to divalent cations. In this study, we observed a preference of manganese over magnesium of PKS18T/D for both autophosphorylation and peptide phosphorylation activity (Fig. 4). PKS18T/D was activated by micromolar amounts of Mn^{2+}, the physiological concentrations in plant cells, indicating possible activity regulation of the kinase by Mn^{2+} *in vivo*. Activation of some kinases by Mn^{2+} has been considered to reflect its involvement in a kinase complex (23). PKS18 may be cytosolic, as suggested by its amino acid sequence. The pH optimum of PKS18T/D activity (Fig. 5*A*) was within the range of cytosolic pH vaules, and was similar to that of a spinach SNF1-like protein kinase (pH between 7.0 and 7.5 in the presence of 2 mM Mg^{2+}) (24). PKS18 phosphorylated two serine-containing peptides but not the threonine-containing peptide (Fig. 5*B*). SOS2 did not phosphorylate commonly used protein substrates, such as myelin basic protein, histone H1, and casein, but did phosphorylate these peptide substrates (9). These observations suggest that the PKS isoforms have strict substrate selectivity. In this study, p3 (ALARAASAAALARRR) was found to be the preferred peptide substrate for PKS18T/D. A synthetic peptide, AMARA (AMARAASAAALARRR), which contains the (hydrophobic)-*X*-(basic)-*X*-*X*-Ser-*X*-*X*-*X*-(hydrophobic) residue, was found to be a minimal recognition motif (25) for a cauliflower AMPK/SNF1 homologue (26). This peptide was also used in the purification of two SNF1-like protein kinases from spinach leaves (27). Therefore, the presence of the hydrophobic and basic residues may be a determinant for the specific substrate of the PKS. However, further systematic analysis of phosphorylation motifs using a series of variants of the p3 peptide is needed to define the importance of these residues for each PKS isoform. In this study, we found that PKS18T/D was slightly inhibited by high concentrations of ATP. ATP inhibition has been demonstrated in other kinases, such as the phosphofructo-1-kinase (PFK) (28). Mammalian PFK has a separate ATP inhibition site (29), whereas PFK from *E. coli* shows a mechanism-based, nonallosteric inhibition by ATP (30). The mechanism of ATP inhibition in PKS18 is still unclear. In addition, some protein kinases are known to utilize GTP as well as ATP as a phosphate donor (31). Whether PKS18 has distinct phosphate donor specificity is unclear.

SOS2 plays a specific role in plant adaptation to high sodium and low potassium stresses (4). Different members of the kinase subfamily could have distinct roles in plants. In this study, we investigated PKS18 function *in vivo* by both overexpression and loss-of-function approaches. Overexpression of PKS18 might affect the functions of other PKSes, and thus overexpression phenotypes need to be interpreted with caution. We therefore further confirmed PKS18 function by using RNAi to silence *PKS18* gene expression. The ABA hypersensitive phenotype of the transgenic plants overexpressing *PKS18T/D* and ABA hyposensitive phenotype of *PKS18*-silenced plants provide a strong case for the involvement of PKS18 in ABA

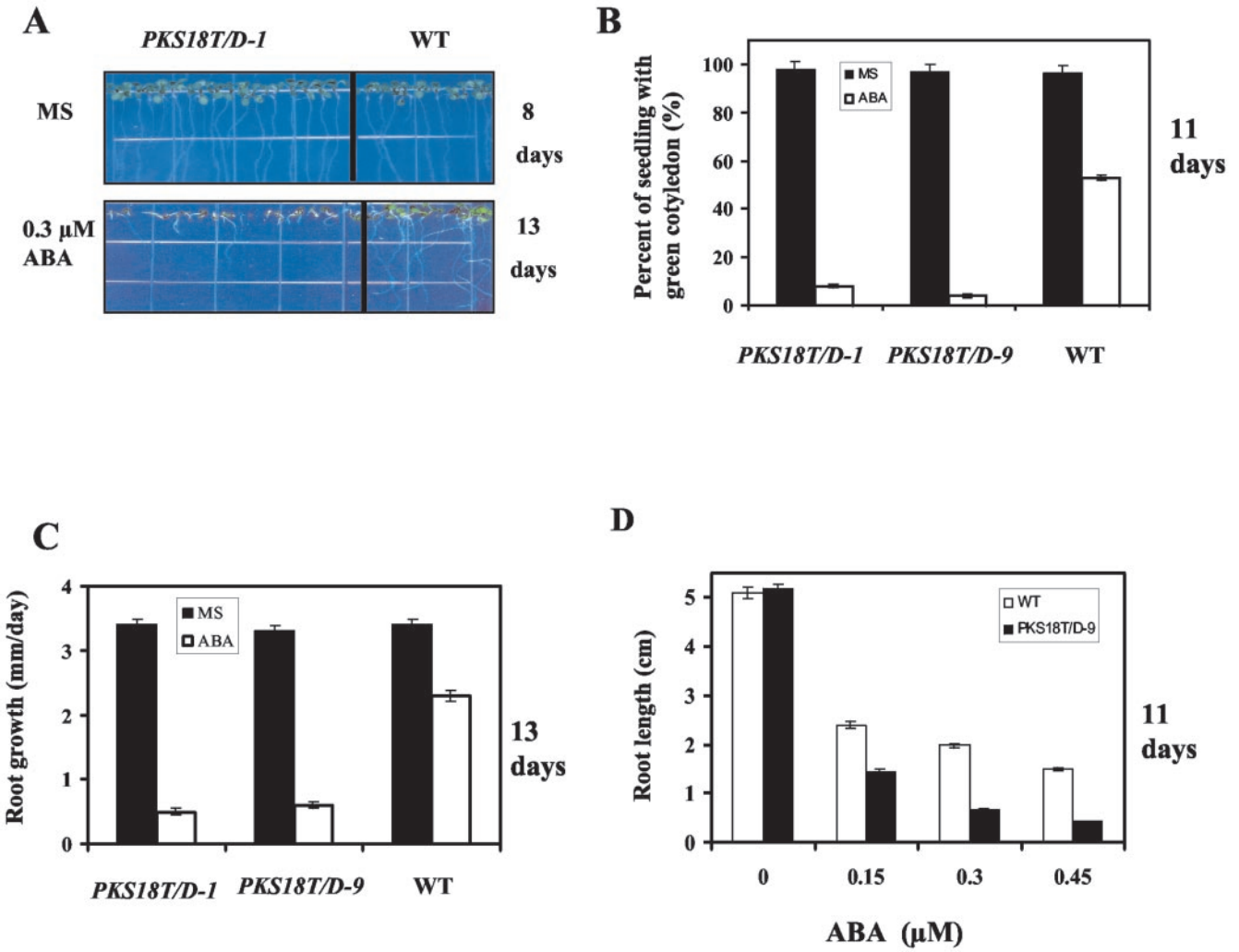

FIG. 8. **ABA sensitivity of seed germination and seedling growth of the transgenic *Arabidopsis* plants overexpressing *PKS18T/D*.** *A*, growth of homozygous transgenic *Arabidopsis* plants (*PKS18T/D*-1) and untransformed control plants (*WT*) on MS agar plates containing 0 μM (MS only) and 0.3 μM ABA, respectively. Seeds were germinated and grown for 8–13 days after seed imbibition. Wild type control plants (*right*) are shown for comparison. *B*, percentage of seedlings with green cotyledons. Seeds of *PKS18T/D*-1 and *PKS18T/D*-9 transgenic plants were germinated and grown for 11 days on ABA-free or 0.3 μM ABA plates, and seedlings with green cotyledons were counted for each treatment. *C*, quantitation of root growth. Seeds were germinated and grown for 13 days on ABA-free or 0.3 μM ABA MS agar plates. The experiments were performed at least three times, and the results of two typical transgenic lines, *PKS18T/D*-1 and *PKS18T/D*-9, are shown here. *D*, ABA dose response of root growth of *PKS18T/D*-9. Seeds were germinated and grown for 11 days on different concentrations of ABA as indicated, and root length was measured at each ABA concentration. These experiments were performed at least three times with similar results. *Error bars* represent S.D. from 10 to 20 samples.

signaling pathway *in vivo* (Figs. 8 and 9). Our results demonstrate an important role of the SnRK3 protein kinase subgroup in plant ABA signaling pathway.

A SnRK2 protein kinase, PKABA1, has been found to be involved in ABA signaling in wheat (32). *PKABA1* was transcriptionally up-regulated by ABA (32), and this kinase may suppress gibberellic acid induced gene expression during cereal grain germination (33). Another Ser/Thr protein kinase gene (*Esi47*) from wheatgrass might also be involved in the same signaling pathway as that for *PKABA1* (34). A guard cell-specific, ABA-activated *Vicia faba* Ser/Thr protein kinase, AAPK, has been shown to control the activity of plasma membrane anion channels (35). Two *Arabidopsis* protein Ser/Thr phosphatase 2C-type genes, *ABI1* and *ABI2* (*ABA-insensitive 1* and *2*), are known to function in controlling plant ABA sensitivity during seed germination and vegetative growth (36–38). Some of the protein kinases in ABA signaling may interact with the ABI phosphatases. An *Arabidopsis* protein phosphatase is known to interact with a Ser/Thr receptor-like kinase (39). These and our results strongly support the notion that protein phosphorylation plays an important role in ABA signaling pathway in plants.

Recent studies have identified a number of transcription factors such as ABI5 and AREBs that are phosphorylated in response to ABA (40–42). The constitutive overexpression of the ABRE (ABA-responsive elements) binding factor, ABF3 or ABF4, in *Arabidopsis* resulted in ABA hypersensitivity phenotypes (43), although the gene knockout/silencing phenotype of either of them is not known yet. Whether the function of PKS18 in plant ABA signaling is mediated by phosphorylating and activating these transcription factors is not known. The involvement of a PKS protein in ABA signaling is not surprising as the PKS family of kinases are known to interact with the SOS3 subfamily of calcium sensors, and as such are involved in calcium signaling (5). Although the calcium sensor(s) that interacts with PKS18 has yet to be identified, the presence of a FISL motif in PKS18 suggests that this kinase binds to one or more of the calcium sensors (5). Ca^{2+} is a second messenger mediating cellular responses to ABA (37). ABA has been recently found to activate multiple Ca^{2+} fluxes in stomatal guard

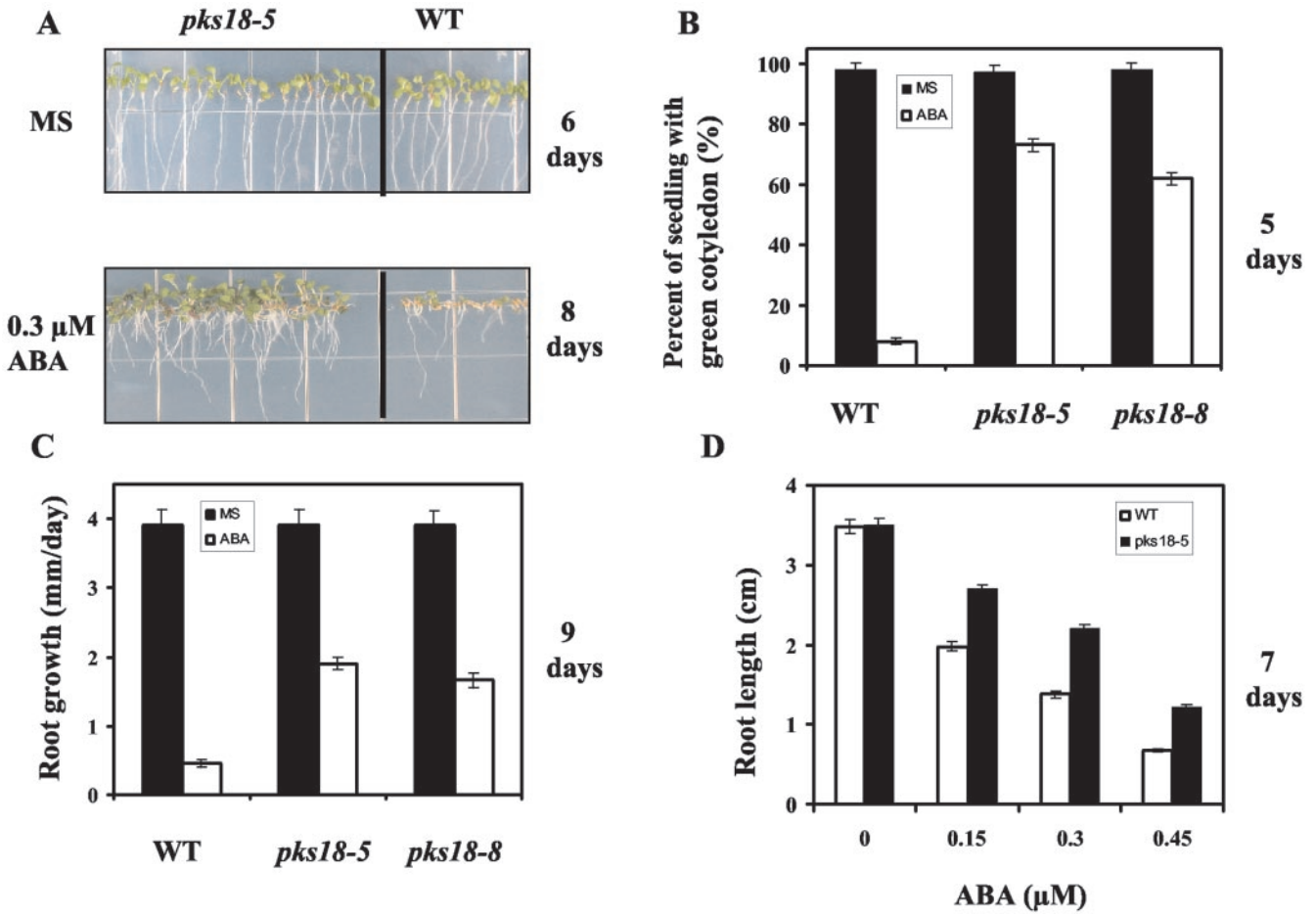

FIG. 9. **ABA sensitivity of *pks18* RNAi lines in seed germination and seedling growth.** *A*, growth of homozygous RNAi plants (*pks18-5*) and untransformed control plants (*WT*) on MS agar plates containing 0 μM (MS only) and 0.3 μM ABA. Seeds of *pks18-4* and *pks18-5* RNAi plants were germinated and grown for 6–10 days after seed imbibition. Wild type control plants (*right*) are shown for comparison. *B*, percentage of seedlings with green cotyledons. Seeds of *pks18-4* and *pks18-5* plants were germinated and grown for 5 days on ABA-free or 0.3 μM ABA plates, and seedlings with green cotyledons were counted for each treatment. *C*, quantitation of root growth. Seeds were germinated and grown for 8 days on ABA-free or 0.3 μM ABA plates, and root length was measured in the wild type and *pks18-5* and *pks18-8* plants. *D*, ABA dose response of root growth in *pks18-5* plants. Seeds were germinated and grown for 7 days on different concentrations of ABA as indicated, and root length was measured at each ABA concentration. These experiments were performed at least three times with similar results. *Error bars* represent S.D. from 10 to 20 samples.

cells in *Commelina communis* (44). ABA treatment might result in a strong and transient increase in cytosolic [Ca^{2+}], which may be perceived by a specific calcium sensor(s). Therefore, we propose that PKS18 functions in mediating calcium signaling in response to ABA signals. Identification of PKS18 interacting partners and substrate proteins will help clarify the precise role of this kinase in ABA signaling pathway in plants. Additionally, it is possible that PKS18 may control plant responses to external ABA by regulating the phosphorylation state of an ABA transport system either in the plasma membrane or vacuole. We have recently demonstrated that SOS2 phosphorylates and regulates the activity of the plasmas membrane sodium/proton antiporter SOS1 (45).

REFERENCES

1. Roberts, D. M. (1993) *Curr. Opin. Cell Biol.* **5,** 242–246
2. Zhao, Y., Pokutta, S., Maurer, P., Lindt, M., Franklin, R. M., and Kappes, B. (1994) *Biochemistry* **33,** 3714–3721
3. *Arabidopsis* Genome Initiative (2000) *Nature* **408,** 796–815
4. Liu, J., Ishitani, M., Halfter, U., Kim, C.-S., and Zhu, J.-K. (2000) *Proc. Natl. Acad. Sci. U. S. A.* **97,** 3730–3734
5. Guo, Y., Halfer, U., Ishitani, M., and Zhu J.-K. (2001) *Plant Cell* **13,** 1383–1399
6. Kreis, M., and Walker, J. C. (2000) *Plant Protein Kinases*, pp. 1–44, Academic Press, San Diego
7. Liu, J., and Zhu, J.-K. (1998) *Science* **280,** 1943–1945
8. Ishitani, M., Liu, J., Halfter, U., Kim, C.-S., Wei, M., and Zhu, J.-K. (2000) *Plant Cell* **12,** 1667–1677
9. Halfter, U., Ishitani, M., and Zhu, J.-K. (2000) *Proc. Natl. Acad. Sci. U. S. A.* **97,** 3735–3740
10. Shi, H., Ishitani, M., Kim, C.-S., and Zhu, J.-K. (2000) *Proc. Natl. Acad. Sci. U. S. A.* **97,** 6896–6901
11. Qiu, Q.-S., Guo, Y., Dietrich, M. A., Schumaker, K. S., and Zhu, J.-K. (2002) *Proc. Natl. Acad. Sci. U. S. A.* **99,** 8436–8441
12. Murashige, T., and Skoog, F. (1962). *Physiol. Plant* **15,** 473–497
13. Wu, S., Ding, L., and Zhu, J-K. (1996) *Plant Cell* **8,** 617–627
14. Shi, H, Xiong, L., Stevenson, B., Lu, T., and Zhu, J.-K. (2002) *Plant Cell* **14,** 575–588
15. Zhu, J.-K., Liu, J., and Xiong, L. (1998) *Plant Cell* **8,** 1181–1191
16. Narasimhulu, S. B., Deng, X., Sarria, R., and Gelvin, S. B. (1996) *Plant Cell* **8,** 873–886
17. Clough, S. J., and Bent, A. F. (1998) *Plant J.* **16,** 735–743
18. Sun, G., and Budde, R. J. (1997) *Biochemistry* **36,** 2139–2146
19. Huse, M., and Kuriyan, J. (2002) *Cell* **109,** 275–282
20. McCartney, R. R., and Schmidt, M. C. (2001) *J. Biol. Chem.* **276,** 36460–36466
21. Waldron, R. T., Rey, O., Iglesias, T., Tugal, T., Cantrell, D., and Rozengurt, E. (2001) *J. Biol. Chem.* **276,** 32606–32615
22. Sturany, S., Lint, J. V., Muller, F., Wilda, M., Hameister, H., Hocker, M., Brey, A., Gern, U., Vandnhede, J., Gress, T., Adler, G., and Seufferlein, T. (2001) *J. Biol. Chem.* **276,** 3310–3318
23. Su, J. Y., Eriksob, E., and Maller, J. L. (1996) *J. Biol. Chem.* **271,** 14430–14437
24. Toroser, D., Plaut, Z., and Huber, S. C. (2000) *Plant Physiol.* **123,** 403–411
25. Dale, S., Wilson, W. A., Edelman, A. M., and Hardie, D. G. (1995b) *FEBS Lett.* **361,** 191–195
26. Ball, K. L., Barker, J., Halford, N. G., and Hardie, D. G. (1995) *FEBS Lett.* **377,** 189–192
27. Sugden, C., Donaghy, P. G., Halford, N. G., and Hardie, D. G. (1999) *Plant Physiol.* **120,** 257–274
28. Tuininga, J. E., Verhees, C. H., Oost, J. V. V., Kengen, S. W. M., Stams, A. J. M., and Vos, W. M. D. (1999) *J. Biol. Chem.* **274,** 21023–21028
29. Kemp, R. G., and Krebs, E. G. (1967) *Biochemistry* **6,** 423–434
30. Zheng, R. G., and Kemp, R. G. (1992) *J. Biol. Chem.* **267,** 23640–23645
31. Muranaka, T., Banno, H., and Machida, Y. (1994) *Mol. Cell. Biol.* **14,** 2958–2965

32. Andeberg, R. J., and Walker-Simmons, M. K. (1992) *Proc. Natl. Acad. Sci. U. S. A.* **89,** 10183–10187
33. Gomez-Cadenas, A., Verhey, S. D., Holappa, L. D., Shen, Q., Ho, D., and Walker-Simmons, M. K. (1999) *Proc. Natl. Acad. Sci. U. S. A.* **96,** 1767–1772
34. Shen, W., Gómez-Cadenas, A., Routly, E. L., Ho, T.-H. D., Simmonds, J. A., and Gulick, P. J. (2001) *Plant Physiol.* **125,** 1429–1441
35. Li, J., Wang X.-Q., Waston M. B., and Assmann S. M. (2000) *Science* **287,** 300–303
36. Koornneef, M., Leon-Kloosterziel, K., Schwartz, S. H., and Zeevaart, J. A. D. (1998) *Plant Physiol. Biochem.* **36,** 83–89
37. Leung, J., and Giraudat, J. (1998) *Annu. Rev. Plant Physiol. Plant Mol. Biol.* **49,** 199–222
38. McCourt, P. (1999) *Annu. Rev. Plant Physiol. Plant Mol. Biol.* **50,** 219–243
39. Stone, J. M., Collinge, M. A., Smith, R. D., Horn, M. A., and Walker, J. C. (1994) *Science* **266,** 793–795
40. Finkelstein, R. R., and Lynch, T. J. (2000) *Plant Cell* **12,** 599–610
41. Uno Y., Furihata T., Abe H., Yoshida R., Shinozaki, K., and Yamaguchi-Shinozaki, K. (2000) *Proc. Natl. Acad. Sci. U. S. A.* **97,** 11632–11637
42. Lopez-Molina, L., Mongrand, S., and Chua, N.-H. (2001) *Proc. Natl. Acad. Sci. U. S. A.* **98,** 4782–4787
43. Kang, J., Choi, H., Im, M., and Kim, S. Y. (2002) *Plant Cell* **14,** 343–357
44. MacRobbie, E. A. C. (2000) *Proc. Natl. Acad. Sci. U. S. A.* **97,** 12361–12368
45. Quintero, F. J., Ohta, M., Shi, H., Zhu, J.-K., and Pardo, J. M. (2002) *Proc. Natl. Acad. Sci. U. S. A.* **99,** 9061–9066